Molecular Omics

ROYAL SOCIETY OF CHEMISTRY

REVIEW

View Article Online
View Journal | View Issue

Cite this: *Mol. Omics*, 2025, **21**, 536

Mass spectrometry-based profiling of phosphoinositide: advances, challenges, and future directions

Yuki Ishino, Yuta Shimanaka, Junken Aoki and Nozomu Kono *

Phosphoinositides (PIPs), the phosphorylated derivatives of phosphatidylinositol (PI), are low-abundance yet critical components of eukaryotic membranes. They play pivotal roles in a wide array of cellular processes, including signal transduction, membrane trafficking, and cell motility. The seven PIP subclasses, generated by phosphorylation at the 3-, 4-, and 5-positions of the inositol ring, are tightly regulated in both spatial and temporal contexts. Dysregulation of PIP metabolism is associated with a range of diseases, including cancer, myopathy, and neurodegenerative and developmental disorders. While the importance of phosphorylation of the inositol ring is well established, recent studies have clarified the role of the fatty acyl chain composition of PIPs. This has resulted in a growing interest in analytical techniques that can determine fatty acyl chain profiles of PIPs. Over the past three decades, substantial advances have been made in mass spectrometry-based techniques, enabling detailed characterization of PIP molecular species, including their phosphate regioisomers. This review provides an overview of the development of mass spectrometric methods for analyzing PIPs, with a particular focus on those enabling the separation of PIP regioisomers and the profiling of their acyl chain composition.

Received 31st May 2025,
Accepted 9th September 2025

DOI: 10.1039/d5mo00115c

rsc.li/molomics

Introduction

Phosphoinositides (PIPs), which are phosphorylated derivatives of phosphatidylinositol (PI), are minor yet crucial components of eukaryotic membranes, playing critical roles in regulating diverse cellular processes. Phosphorylation at the 3-, 4-, and 5-positions of the inositol ring generates seven distinct PIP subclasses: PI(3)P, PI(4)P, PI(5)P, PI(3,4)P_2, PI(3,5)P_2, PI(4,5)P_2, and PI(3,4,5)P_3 (Fig. 1A). Each subclass exhibits a unique subcellular distribution: PI(4,5)P_2 is predominantly localized to the plasma membrane; PI(4)P to the Golgi apparatus and plasma membrane; PI(3,5)P_2 to late endosomes and lysosomes;

Laboratory of Health Chemistry, Graduate School of Pharmaceutical Sciences, the University of Tokyo, Hongo 7-3-1, Bunkyo-ku, Tokyo 113-0033, Japan.
E-mail: nozomu@mol.f.u-tokyo.ac.jp; Fax: +81-3-3818-3173; Tel: +81-3-5841-1076

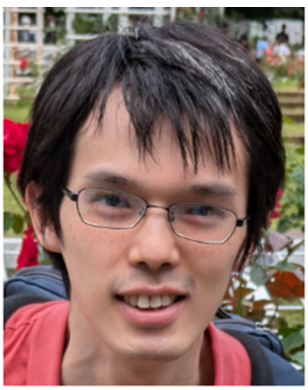

Yuki Ishino

Yuki Ishino received his PhD degree in Pharmaceutical Science from the University of Tokyo and is currently a project research fellow in the Laboraotry of Health Chemistry, Graduate School of Pharmaceutical Sciences at the University of Tokyo. His research focuses on the roles of arachidonic acid-containing phosphatidylinositol and phosphoinositides in mammalian tissues, especially in developing mouse brain.

Nozomu Kono

Nozomu Kono received his PhD in Pharmaceutical Sciences from the University of Tokyo in 2007 under the supervision of Prof. Hiroyuki Arai. He is currently an Associate Professor at the Graduate School of Pharmaceutical Sciences, University of Tokyo. He has also carried out research at the Cambridge Institute for Medical Research with Prof. David Ron. His research focuses on the physiological and pathological roles of fatty acyl chains in membrane phospholipids, with particular interest in lipotoxicity and phosphatidylinositol remodeling.

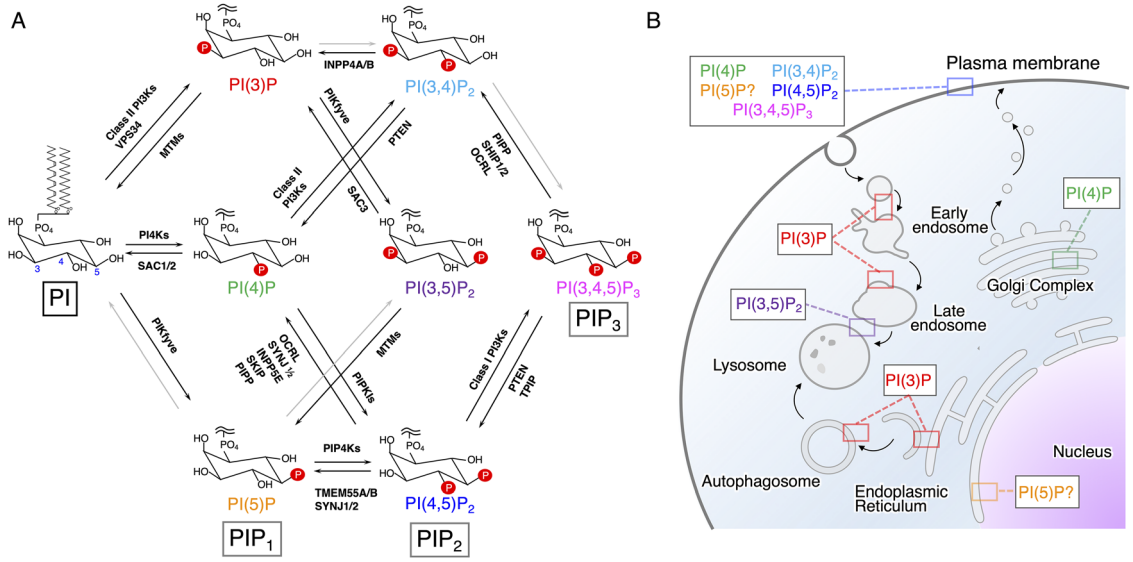

Fig. 1 Metabolism and subcellular localization of phosphoinositides. (A) Chemical structure of PI and PIPs. For PIPs, only the polar heads are shown. The addition and removal of phosphate groups at the 3′-hydroxy, 4′-hydroxy, and 5′-hydroxy groups of PI by phosphoinositide kinases and phosphatases create seven distinct PIP subclasses. (B) Subcellular localization of PIPs. The spatiotemporally controlled activity of phosphoinositide kinases and phosphatases creates a distinctive enrichment of PIPs across the cellular compartments: PI(3)P, enriched in early/late endosomes and autophagosome, is involved in vesicle transport and autophagy; PI(4)P, localized mainly to the Golgi complex and plasma membrane, contributes to Golgi complex formation and lipid transport; PI(5)P, found in the plasma membrane and nucleus, participates in stress responses and transcriptional regulation; $PI(4,5)P_2$ and $PI(3,4)P_2$, enriched in the plasma membrane, regulate signal transduction, endocytosis, and cell polarity; $PI(3,4,5)P_3$, also at the plasma membrane, promotes cell survival and proliferation; and $PI(3,5)P_2$, localized to late endosomes and lysosomes, is involved in lysosomal regulation.

and PI(3)P to early and late endosomes[1,2] (Fig. 1B). PI(3)P is also synthesized at the endoplasmic reticulum during autophagy initiation. $PI(3,4)P_2$ and $PI(3,4,5)P_3$ are produced transiently at the plasma membrane in response to extracellular stimuli. Although the precise localization of PI(5)P is unclear, it has been detected at the plasma membrane, early endosomes, and within the nucleus.[3]

The spatial distribution of PIPs is tightly regulated by the coordinated actions of specific lipid kinases and phosphatases (Fig. 1A). At distinct subcellular locations, PIPs act as molecular landmarks that orchestrate the recruitment and activity of effector proteins involved in key cellular processes such as cell migration, adhesion, signal transduction, and membrane trafficking[2] (Fig. 1B). Classically, $PI(4,5)P_2$ serves as a precursor of the second messengers inositol-1,4,5-trisphosphate (IP_3) and diacylglycerol (DAG), which are produced *via* phospholipase C-mediated hydrolysis of $PI(4,5)P_2$ in response to extracellular stimuli.[4] Recently, PI(4)P has also been recognized as a central regulator of intracellular lipid transport.[2]

Dysregulation of PIP metabolism has been increasingly recognized as a key contributor to a broad spectrum of human diseases.[2,4] For instance, somatic activating mutations in PIK3CA, which encodes a class I PI3-kinase responsible for generating $PI(3,4,5)P_3$, have been identified in breast, endometrial, colorectal, urinary tract, and ovarian cancers.[5,6] PTEN, which encodes an inositol 3-phosphatase that dephosphorylates $PI(3,4,5)P_3$, is frequently mutated in cancers such as glioblastoma, endometrial, and prostate cancers.[6,7] Mutations in OCRL1, which encodes an inositol-5-phosphatase acting on $PI(4,5)P_2$ and $PI(3,4,5)P_3$, cause Lowe syndrome, an X-linked disorder characterized by congenital cataracts, intellectual disability, and renal failure.[8] Mutations in MTM1, which affect an inositol 3-phosphatase that dephosphorylates PI(3)P and $PI(3,5)P_2$, lead to X-linked myotubular myopathy.[9] Mutations in MTMR2, another inositol 3-phosphatase targeting PI(3)P and $PI(3,5)P_2$, are associated with Charcot-Marie-Tooth disease 4B1, a severe autosomal recessive demyelinating neuropathy.[10]

Increasing evidence indicates that PIP acyl chains influence the biological functions of PIPs. The acyl chain composition of PIPs affects Akt phosphorylation activity of PDK1,[11] activation of potassium channel GIRK1/GIRK4,[12] membrane binding of HIV-1 Gag protein,[13] lipid transfer activity of Osh6p,[14] and the coactivator peptide-binding affinity of SF-1.[15] The acyl chain composition of PIPs also impacts the biophysical properties of membranes, including the formation of PIP-enriched nanodomains, which in turn influence membrane curvature[16] and PIP metabolism.[17,18] Moreover, PIP_2 species with saturated acyl chains potentiate effector T cell signaling.[19] Alterations in PI/PIP acyl chain profiles have been associated with tumorigenesis, raising the possibility that cancer cells exploit specific PIP molecular species to rewire signaling networks.[20–22] These findings underscore the need for comprehensive PIP profiling that captures both head group phosphorylation and fatty acyl chain identity.

Traditional methods for PIP measurement have relied on metabolic labeling with [^{3}H]inositol or [^{32}P]phosphate, followed by deacylation and separation of PIP subclasses using

high-performance liquid chromatography (HPLC) methods that separate by headgroup polarity.[23] The radiolabeling methods revealed that the total PIP content is less than 10% of PI, which itself comprises 5–10% of the total phospholipids, with PI(4)P and PI(4,5)P_2 being the major species detected.[23] However, these methods do not allow for the quantification of endogenous PIP levels and thus are not applicable to tissue samples. Alternative non-radioactive methods, such as ELISA-based mass assays using PIP-binding domains and PIP kinase-based mass assays,[24–26] can quantify endogenous PIP subclasses, but they do not provide information on fatty acyl chain composition.

Electrospray ionization mass spectrometry (ESI-MS) is a powerful and widely used technique for quantifying individual lipid species with high sensitivity.[27,28] Over the past three decades, substantial methodological advances have enabled the precise quantification of PIP molecular species, which includes information about fatty acyl chains. More recently, innovations have enabled the discrimination of PIP_1 and PIP_2 regioisomers, along with their fatty acyl chain profiles. In this review, we provide an overview of historical and current mass spectrometry methods of PIP analysis (Table 1) and discuss where further technical innovations are needed.

ESI-MS analysis of intact PIPs

The first application of ESI-MS to the analysis of PIP_1 and PIP_2 was demonstrated by Michelsen *et al.*[29] They successfully quantified 1-stearoyl-2-arachidonoyl (18 : 0_20 : 4) species of PIP_1 and PIP_2 in bovine brain extracts. Using single-ion monitoring in negative-ion mode, they detected approximately 200 pmol of each species. Hsu *et al.*[30] investigated the fragmentation mechanisms of PI(4)P and PI(4,5)P_2 using collision-activated dissociation (CAD) in tandem ESI-MS (ESI-MS/MS), showing that ESI-MS/MS is a powerful tool for structural

Table 1 Advances in the analysis of PIPs by mass spectrometry

Authors	Year	Advances/novelty	Method	Derivatization	Regioisomer separation	Ref.
Michelsen *et al.*	1995	Application of ESI-MS to PIP_1 and PIP_2 analysis.	ESI-MS	No	—	29
Hsu *et al.*	2000	The detailed mechanism of fragmentation of PI(4)P and PI(4,5)P_2 ions under CAD with ESI-MS/MS.	ESI-MS/MS	No	—	30
Wenk *et al.*	2003	Measurement of PIP_1 and PIP_2 acyl profiles in biological samples by ESI-MS/MS. Enhancement of PIPs signal intensities by piperidine.	ESI-MS/MS	No	—	31
Milne *et al.*	2005	Measurement of PI(3,4,5)P_3 molecular species in biological samples. Development of 2-step extraction method.	ESI-MS	No	—	32
Pettitt *et al.*	2006	Measurement of PIP molecular species and PIP_2 regioisomers by normal phase LC-MS. Development of buffered citrate extraction method. Use of ethylamine as a mobile phase modifier. Distinct fragmentation pattern of PI(4)P from other PIP_1s at MS^3.	NPLC-ESI-MS ESI-MS^n	No	PIP_2 and PI(4)P	33
Ogiso *et al.*	2008	Measurement of PIP molecular species by reverse phase LC-MS. Use of DEAE column to obtain a PIP-rich fraction.	RPLC-ESI-MS/MS	No	—	34
Clark *et al.*	2011	Development of PIP derivatization method with TMS-diazomethane. Measurement of methylated PIPs by LC-MS/MS.	RPLC-ESI-MS/MS	Yes	—	35
Wang *et al.*	2016	Development of a method for quantifying each PIP_2 regioisomer and PI(3)P by simulation using the information of methylation patterns.	ESI-MS/MS	Yes	PIP_2 and PI(3)P	37
Kim *et al.*	2017	Development of LC-MS/MS method for structural identification of *sn*-1 and *sn*-2 fatty acyl chains of PIPs. Enhancement of PIPs signal intensities by ammonium ion adduction.	RPLC-ESI-MS/MS	Yes	—	36
Malek *et al.*	2017	Development of a method to distinguish between 18 : 0/20 : 4 PI(4,5)P_2 and PI(3,4)P_2 in biological samples by shortening the acyl groups of PIPs by ozone cleavage.	RPLC-ESI-MS/MS	Yes	PI(4,5)P_2 and PI(3,4)P_2	39
Bui *et al.*	2018	Development of a technique for measuring non-derivatized PIP_2 regioisomers by RPLC-MS with the addition of the ion-pairing reagents.	RPLC-ESI-MS/MS	Yes	PIP_2	38
Li *et al.*	2021	Development of a method to separate all methylated PIP_1 and PIP_2 regioisomers by LC-MS using a cellulose-based chiral column. Use of SWATH to obtain a comprehensive PIP profile.	RPLC-ESI-MS/MS	Yes	PIP_1 and PIP_2	40
Morioka *et al.*	2022	Development of a method for simultaneously quantifying molecular species of all seven PIP classes by LC-ESI-MS/MS using a cellulose-based chiral column.	RPLC-ESI-MS/MS	Yes	PIP_1 and PIP_2	41
Shimanaka *et al.*	2022	Development of a method for simultaneously quantifying molecular species of all seven PIP classes by SFC-ESI-MS/MS using a β-cyclodextrin column.	SFC-ESI-MS/MS	Yes	PIP_1 and PIP_2	42

characterization of PIPs. Wenk *et al.*[31] were the first to report comprehensive fatty acyl chain profiling of PIP_1 and PIP_2 molecular species in biological samples by ESI-MS/MS. They demonstrated that the addition of piperidine significantly enhanced the negative-mode ionization efficiency of PIP_1 and PIP_2. Using this approach, they found elevated levels of PIP_2 species in fibroblasts derived from patients with Lowe syndrome. They also showed that deficiency of enzymes involved in PIP metabolism, such as Sac1, Pik1, and Vps34, in *Saccharomyces cerevisiae* affects not only the levels of PIPs but also their acyl chain profiles, suggesting that these enzymes exhibit substrate selectivity for specific acyl chains or that organelle-specific PI or PIP acyl chain composition may exist at the sites where these enzymes localize. Milne *et al.*[32] further extended the scope of PIP profiling by enabling the quantification of $PI(3,4,5)P_3$, which is the least abundant PIP subclass in vivo, along with PIP_1 and PIP_2. To minimize the interference of other phospholipids during analysis, they developed a selective two-step extraction protocol, in which an initial chloroform/methanol extraction removed unwanted non-polar lipids and a subsequent acidic extraction recovered PIPs from the residual pellet. Their analysis revealed that different profiles of $PI(3,4,5)P_3$ were produced in macrophages stimulated by various agonists, such as lysophosphatidic acid and C5a, suggesting that the activation mechanisms of PI-3 kinase and/or substrate availability among $PI(4,5)P_2$ species vary depending on the agonist.

Wenk *et al.*[31] and Milne *et al.*[32] employed direct infusion mass spectrometry, a technique susceptible to ion suppression effects, which could potentially compromise sensitivity. To address this limitation, Pettitt *et al.*[33] developed a normal phase LC-MS method for PIP profiling. They thoroughly investigated each step, from extraction to final analysis of PIPs, and made several improvements. Especially, they developed a highly efficient buffered citrate extraction method to minimize acid-induced phosphoinositide degradation and a sensitive LC-MS method using ethylamine as a mobile phase modifier. Their approach enabled the detection of PIP_1 in human platelets, with detection limits of 250 fmol for PIP_1, 1 pmol for PIP_2, and 5 pmol for PIP_3.

Reversed-phase (RP) LC is highly effective for separating phospholipid molecular species and detecting low-abundance components. Ogiso *et al.*[34] developed a sensitive RPLC-MS method for profiling the acyl chain composition of PIP_1, PIP_2, and PIP_3. They enriched PIP fractions using (diethylamino)ethyl (DEAE)-cellulose columns and utilized an alkaline-resistant C8 column for separation. Applying this method to epidermal growth factor (EGF)-stimulated A431 cells, they quantified 17 distinct PIP_1 and PIP_2 molecular species, demonstrating that EGF stimulation increased the

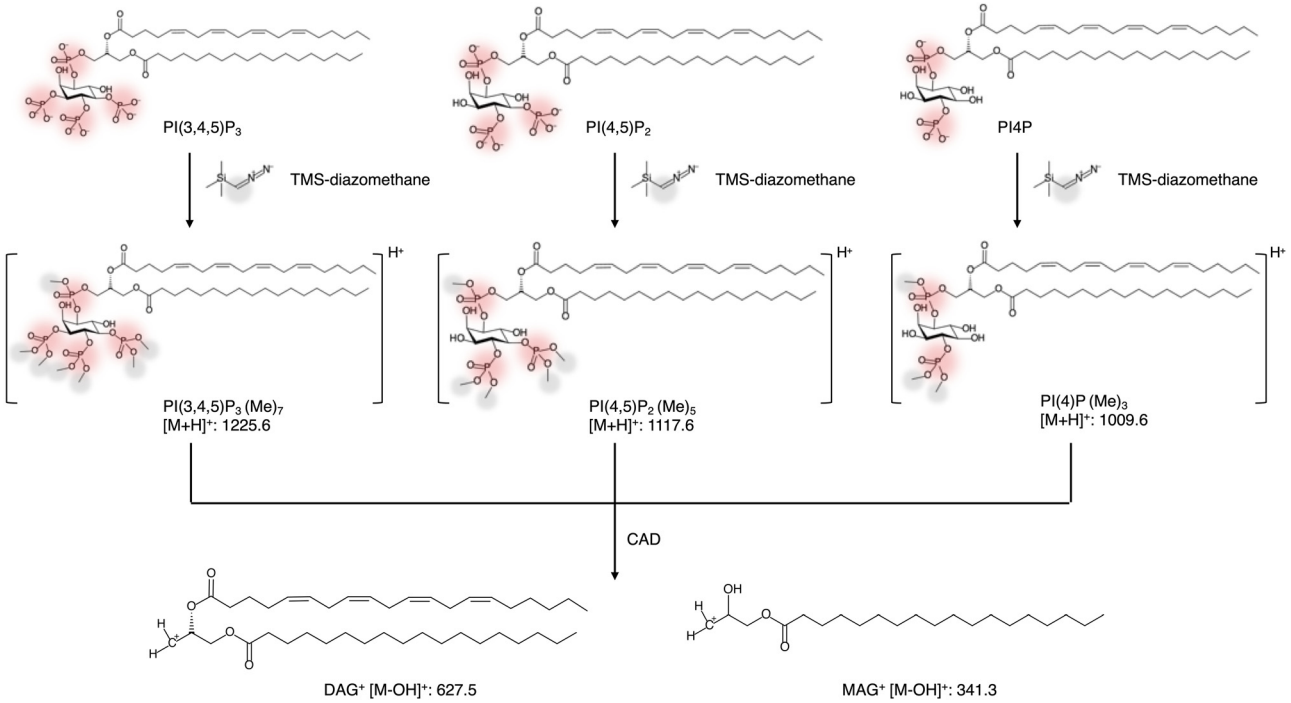

Fig. 2 Methylation of the phosphate groups of PIPs by TMS-diazomethane. Treatment of $PI(3,4,5)P_3$ with TMS-diazomethane yields heptamethylated $PI(3,4,5)P_3$ [$PI(3,4,5)P3\ (Me)_7$]. In the case of PI(4)P and $PI(4,5)P_2$, trimethylated PI(4)P [$PI(4)P\ (Me)_3$] and pentamethylated $PI(4,5)P_2$ [$PI(4,5)P_2\ (Me)_5$] are mainly produced, respectively. The methylated PIPs are readily detected as positive ions, and collision-activated dissociation (CAD) of a methylated PIP ion yields a diacylglycerol (DAG) ion and a monoacylglycerol (MAG) ion. The DAG ion is useful for the sensitive detection of methylated PIPs in MRM mode, whereas the MAG ion allows determination of the fatty acyl chain compositions of PIPs. TMS-diazomethane also produces overmethylated PIPs, such as tetra- or pentamethylated PIP_1 and hexa- or heptamethylated PIP_2, and the proportion of overmethylated PIPs can be used to discriminate between PIP_1 and PIP_2 regioisomers. Chemical structures were drawn using Marvin Sketch [19.16.0, Chemaxon (**https://www.chemaxon.com**)].

levels of almost all PIP_1 molecular species without affecting the levels of PIP_2 molecular species. They also showed that levels of 36 : 2 PIP_3, which appears to be the most abundant PIP_3 species, increased in response to EGF stimulation. They achieved a detection limit of 25 fmol for each PIP molecular species.

Improving detection sensitivity of PIPs *via* derivatization

The difficulty in quantifying PIPs arises from (i) their low abundance *in vivo*, (ii) poor ionization efficiency by ESI, and (iii) low extraction efficiency. Notably, the low recovery efficiency and poor quantification reproducibility of PIPs are largely due to the adsorption of acidic phosphate head groups on glass and metal surfaces and their susceptibility to hydrolysis.[33,34] To address these issues, Clark *et al.*[35] developed a derivatization method in which phosphate groups are methylated using trimethylsilyl (TMS)-diazomethane (Fig. 2). Derivatization can be performed directly in the acidified chloroform-methanol extracts from cells or tissues and is completed within 10 minutes. This reaction introduces three, five, and seven methyl groups to PIP_1, PIP_2, and PIP_3, respectively (Fig. 2). Methylation improves the recovery and chemical stability of PIPs and reduces their net negative charge. The methylated PIPs can be detected as positive ions *via* ESI-MS, and CAD of these methylated ions induces neutral loss of the methylated inositol phosphate headgroup, yielding charged diacylglycerol fragments. To further improve sensitivity for the low-abundance PIP_3, Clark *et al.* concentrated methylated PIP_3 using a C4 RPLC column and detected it *via* neutral loss scan or multiple reaction monitoring (MRM), targeting the diacylglycerol fragment ions as Q3 masses. Utilizing this approach, they were able to quantify PI(3,4,5)P_3 species in fMLP-stimulated human neutrophils, glucose-stimulated human adipose tissue, and insulin-stimulated mouse liver. Notably, they demonstrated selective accumulation of 18 : 0/20 : 4 PI(3,4,5)P_3 in EGF-stimulated MCF10a breast cancer cells even though its precursor, 18 : 0/20 : 4 PI(4,5)P_2, is the least abundant PI(4,5)P_2 species.

Kim *et al.*[36] developed an LC-MS/MS method for structurally characterizing the *sn*-1 and *sn*-2 fatty acyl chains of PIPs. They discovered that CAD of methylated PIPs generates *sn*-1 monoacylglycerol ions. Then, using positive ion mode, they performed precursor ion scans targeting these fragments, and neutral loss scans of the inositol headgroup. By comparing the LC retention times obtained from the two scan modes, they were able to determine the fatty acyl chains at the *sn*-1 and *sn*-2 positions. Furthermore, they found that ammonium adduction enhanced PIP signal intensities approximately twofold. Using this technique, they were able to quantitatively profile PIP species in insulin-treated AML12 hepatocytes and mouse liver with structural information of the *sn*-1 and *sn*-2 fatty acyl chains.

Development of chromatographic separation of PIP_1 and PIP_2 regioisomers

Since each PIP_1 and PIP_2 regioisomer plays a distinct role in cellular functions, the separation and quantification of individual regioisomers are crucial for understanding their specific biological roles. However, since PIP regioisomers have identical masses, they cannot be distinguished by mass spectrometry alone. Pettitt *et al.* addressed this issue by developing a method to analyze non-derivatized PIP regioisomers using normal-phase LC coupled with ion trap mass spectrometry.[33] They demonstrated that the three PIP_2 regioisomers could be separated using a silica column under normal-phase conditions. While the three PIP_1 regioisomers could not be completely resolved by LC alone, PI(5)P eluted slightly earlier than PI(3)P and PI(4)P. Furthermore, they found that the MS^3 fragmentation pattern of PI(4)P differed from those of PI(3)P and PI(5)P, enabling estimation of the relative abundance of PI(4)P among the PIP_1 isomers. By combining chromatographic separation and diagnostic MS fragmentation, they successfully quantified each PIP_1 regioisomer.

Wang *et al.*[37] found that the percentage of overmethylated PIPs produced in the reaction with TMS-diazomethane varied among PIP_2 regioisomers and used the values to quantify each PIP_2 regioisomer. For PIP_1, only PI(3)P could be distinguished from PI(4)P and PI(5)P, as the latter two shared the same methylation pattern. Using this technique, they revealed alterations in PIP profiles in the cerebral cortex of *db/db* mice. Bui *et al.*[38] reported a method for separating non-derivatized PIP_2 regioisomers using C18 RPLC with diisopropylethanolamine (DiiPEA) and EDTA as ion-pairing agents. Melek *et al.*[39] used an innovative approach to distinguish between 18 : 0/20 : 4 PI(4,5)P_2 and PI(3,4)P_2 in biological samples by shortening the acyl chain through ozone-induced cleavage. Thus, while various efforts have been made to analyze individual PIP regioisomers, there remains a strong interest in developing a simple and versatile method capable of separating and simultaneously quantifying all PIP regioisomers.

Recently, three independent groups, including ours, have reported methods for the simultaneous analysis of all PIP regioisomers using chromatography-coupled tandem mass spectrometry.[40–42] Li *et al.*[40] successfully separated all methylated PIP_1 and PIP_2 regioisomers using HPLC with a cellulose-based chiral column. They also employed SWATH (sequential window acquisition of all theoretical mass spectra), a data-independent acquisition technique, to obtain a comprehensive PIP profile. Since SWATH comprehensively acquires MS2 spectra of PIPs, including DAG and MAG ions, it enables determination of the fatty acyl chain combinations of PIPs. Using their method, they reported complete PIP profiles of human plasma, *Pichia pastoris*, and HeLa cells, as well as changes in PIP profiles in HeLa cells upon treatment with PI3K inhibitor wortmannin. Morioka *et al.*[41] also developed a method to simultaneously quantify the molecular species of all seven PIP subclasses by HPLC-ESI-MS/MS using a cellulose-based chiral column, employing MRM for sensitive and specific detection. Their method revealed (i) profound changes in acyl chain composition of PI(3,4)P_2 and PI(3,4,5)P_3 in *Pten*-deficient prostate cancerous tissues, (ii) extracellular mobilization of PIPs upon expression of oncogenic PIK3CA, and (iii) the PIP profile of exosomes. Although both methods employed cellulose-based chiral columns, the elution order of the PIP_1 regioisomers

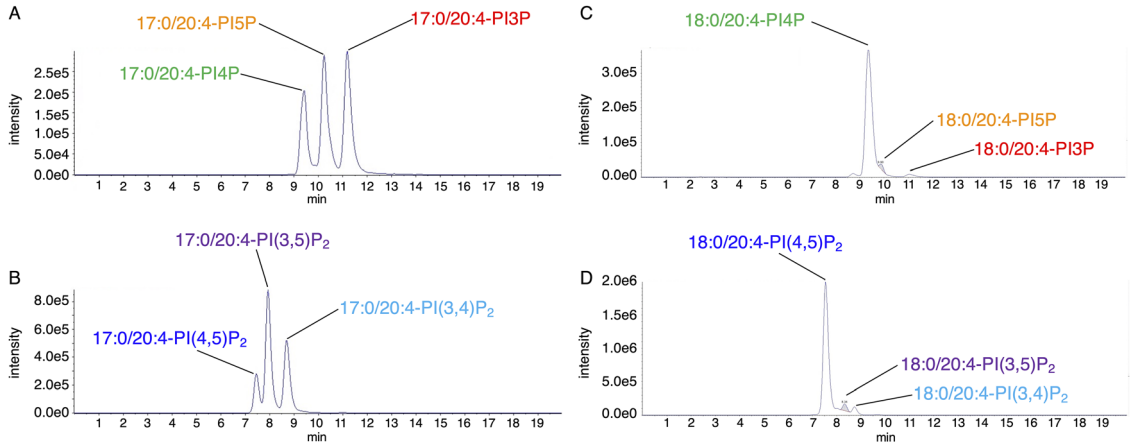

Fig. 3 Separation of PIP_1 and PIP_2 regioisomers by SFC. (A) and (B) Synthetic 1-heptadecanoyl-2-arachidonyl (17 : 0/20 : 4) PIP standards were methylated with TMS-diazomethane and analyzed by SFC-ESI-MS/MS. MRM chromatograms of 17 : 0/20 : 4-PIP_1 (A) and 17 : 0/20 : 4-PIP_2 (B) are shown. PIP_1s are in the order of PI(4)P, PI(5)P and PI(3)P, while PIP_2s are eluted in the order of PI(4,5)P_2, PI(3,5)P_2, and PI(3,4)P_2, respectively. (C) and (D) PIPs were extracted from mice liver, methylated with TMS-diazomethane, and analyzed by SFC-ESI-MS/MS. MRM chromatograms of 1-stearoyl-2-arachidonoyl (18 : 0/20 : 4) PIP_1 (C) or PIP_2 (D). Minor PIP_1s [PI(5)P and PI(3)P] and minor PIP_2s [PI(3,4)P_2 and PI(3,5)P_2] often co-elute on the shoulders of the dominant PI(4)P and PI(4,5)P_2 peaks, respectively, which hinders their accurate quantification.

differed: the orders were PI(3)P, PI(5)P, and PI(4)P in the method of Li *et al.*, and PI(3)P, PI(4)P, and PI(5)P in the method of Morioka *et al.* In both methods, PIP_2 regioisomers eluted in the order PI(3,5)P_2, PI(3,4)P_2, and PI(4,5)P_2.

As an alternative chromatographic approach, we developed a method to separate methylated PIP_1 and PIP_2 regioisomers using supercritical fluid chromatography (SFC).[42] A supercritical fluid is a substance maintained at a temperature and pressure above its critical point. It exhibits gas-like diffusivity and liquid-like solubility, enabling rapid and efficient separation. Importantly, SFC and HPLC have distinct separation behaviors, which makes it possible for SFC to separate compounds that HPLC cannot. We found that SFC using a β-cyclodextrin column effectively separated methylated PIP_1 and PIP_2 regioisomers (Fig. 3). Our SFC-based method provided a distinct elution profile compared to HPLC-based methods: PIP_1 regioisomers eluted in the order PI(4)P, PI(5)P, and PI(3)P, while PIP_2 regioisomers eluted in the order PI(4,5)P_2, PI(3,5)P_2, and PI(3,4)P_2. Furthermore, SFC achieved broader separation windows, enhancing the resolution between regioisomers. Coupling SFC to ESI-MS/MS in MRM mode enabled the measurement of the molecular species of all seven PIP subclasses in biological samples. Using MRM transitions with the monoacylglycerol ion set as Q3, we were also able to detect PIPs with information on their fatty acyl chain combinations. Applying this method to mouse tissues, we discovered that PIPs containing two saturated fatty acids, which were hardly detected in most tissues or cultured cells, were abundant in the testis. We also found that less unsaturated PI(3)P molecular species, such as 34 : 1, 34 : 2, 36 : 1, and 36 : 2 PI(3)P, selectively increased during autophagy induction.

Very recently, SFC-MS-based PIP profiling revealed that impaired production of PI(4,5)P_2 in neural stem cells underlies the microcephaly in *Mboat7* deficiency.[43] LPLAT11, encoded by *Mboat7*, is a lysophospholipid acyltransferase that selectively incorporates arachidonic acid into phosphatidylinositol (PI).[44] In humans, loss-of-function mutations in *MBOAT7* are associated with neurodevelopmental disorders characterized by microcephaly and intellectual disability.[45] Consistently, *Mboat7*-deficient mice exhibit microcephaly.[45–47] We found that *Mboat7* deficiency compromised the integrity of radial glial cells, which are the neural stem cells responsible for cortical development, resulting in reduced proliferation, impaired differentiation into intermediate progenitor cells, and increased apoptosis. These cellular defects were preceded by morphological abnormalities of the Golgi apparatus and reduced E-cadherin expression at the ventricular surface. SFC-MS analysis revealed that a reduction in arachidonic acid-containing species and a reciprocal increase in non-arachidonic acid-containing species occurred across PI, PI(4)P, and PI(4,5)P_2 in *Mboat7* KO cortices. In addition to changes in acyl chain composition, total PI(4,5)P_2 levels were significantly reduced, whereas total PI and PI(4)P levels remained unchanged. This selective decrease is likely due to the acyl chain preference of PIP5Kγ,[48] a key PI(4,5)P_2-producing enzyme in the developing cortex. Furthermore, pharmacological inhibition of PIP5Kγ in wild-type embryonic cortices recapitulated the Golgi abnormalities and E-cadherin reduction observed in *Mboat7* KO cortices. These findings show that PI(4,5)P_2 has a critical role in maintaining radial glial cell integrity during cortical development and underscore the utility of SFC-MS in elucidating PIP-mediated mechanisms in physiology and pathology.

Future perspectives in phosphoinositide analysis

Recent advances have made it possible to measure molecular species in all seven PIP subclasses. This will greatly improve our understanding of the physiological and pathological roles of PIPs. Nevertheless, challenges remain in the absolute quantification of individual PIP species. Because PI(4)P and PI(4,5)P_2 are far more abundant than other PIP classes in biological samples, minor PIP_1s [PI(5)P and PI(3)P] and minor PIP_2s [PI(3,4)P_2 and PI(3,5)P_2] often co-elute on the shoulders of the dominant PI(4)P

Table 2 Comparison of relative abundance of PIPs determined by mass spectrometry and radioisotope labeling

	Cell type			
	Mouse embryonic fibroblasts		HeLa cells	
Method	Methylation followed by SFC-MS	[^{3}H]Inositol-labeling followed by HPLC	Methylation followed by HPLC-MS	[^{3}H]Inositol-labeling followed by HPLC
PI(3)P	9.1	2.2	5.7	2.8
PI(4)P	36.2	37.2	36.1	45.3
PI(5)P	8.1	3.5	7.6	0.8
PI(3,4)P_2	2.6	Not detected	1.9	Not detected
P(3,5)P_2	3.7	0.5	2.7	Not detected
PI(4,5)P_2	40.4	56.6	46.1	51.0
Ref.	Shimanaka *et al.*[42]	Steinfeld *et al.*[49]	Li *et al.*[40]	Sarkes *et al.*[50] & Fujii *et al.*[51]

Values represent % of total PIPs.

and PI(4,5)P_2 peaks, respectively[42] (Fig. 3), hindering their accurate quantification. Indeed, the levels of these minor PIP species measured by HPLC-ESI-MS/MS or SFC-ESI-MS/MS were substantially higher than those determined using traditional radioisotope-labeling techniques[40,42,49–51] (Table 2). While differences in culture conditions during radioisotope labeling may partially account for this discrepancy, it is also possible that minor PIP signals are artificially elevated due to overlap with the abundant PI(4)P and PI(4,5)P_2 peaks. Although peak-integration methods, such as tangential skim, can partially address the overestimation caused by peak overlap, further improvements in the chromatographic separation of PIP regioisomers will be essential to achieve more accurate absolute quantification of PIP molecular species in biological matrices.

Recent advances in mass spectrometry (MS)-based imaging techniques have enabled the visualization of diverse phospholipid species at single-cell resolution within tissues.[52,53] However, there have been only a few reports on MS imaging of PIPs to date,[54,55] and none of them are capable of distinguishing between PIP regioisomers. For MS imaging of PIP regioisomers, it is necessary to separate the regioisomers inside the mass spectrometer. One promising approach for isomer-specific imaging of PIPs is ion mobility spectrometry (IMS), a gas-phase separation technique in which ions are separated base on their collision cross-section (CCS), which reflects differences in molecular size and shape.[56] Even when two isomers have the same mass-to-charge ratio, differences in their CCS values can result in distinct drift times, enabling their separation prior to mass analysis. Moreover, when integrated with LC-ESI-MS/MS or SFC-ESI-MS/MS workflows, IMS provides an additional orthogonal dimension of separation, enhancing the resolution of PIP regioisomers and thereby improving absolute quantification. Incorporating emerging technologies such as IMS into PIP analysis platforms will help overcome current limitations and further advance our understanding of the complex physiological and pathological functions of PIPs.

Conflicts of interest

YS and NK are co-inventors of Japanese Patent 7017704, titled ''biological membrane phosphoinositide separation method.'' All other authors declare no competing interests.

Data availability

No primary research results, software or code have been included and no new data were generated or analyzed as part of this review.

Acknowledgements

This work was supported by Grant-in-Aid for Early-Career Scientists to (18K14898 to YS); by Grants-in-Aid for Scientific Research (B) (23K27125 to NK); by AMED-CREST, AMED (JP 21gm1210013 to NK); and by Moonshot R&D Program (JPMJMS2024-11 and JPMJMS2024-15 to JA).

References

1 L. Picas, F. Gaits-Iacovoni and B. Goud, *F1000 Res.*, 2016, **5**, 422.
2 Y. Posor, W. Jang and V. Haucke, *Nat. Rev. Mol. Cell Biol.*, 2022, **23**, 797–816.
3 J. Hasegawa, B. S. Strunk and L. S. Weisman, *Cell Struct. Funct.*, 2017, **42**, 49–60.
4 T. Balla, *Physiol. Rev.*, 2013, **93**, 1019–1137.
5 J. A. Engelman, J. Luo and L. C. Cantley, *Nat. Rev. Genet.*, 2006, **7**, 606–619.
6 T. L. Yuan and L. C. Cantley, *Oncogene*, 2008, **27**, 5497–5510.
7 L. Salmena, A. Carracedo and P. P. Pandolfi, *Cell*, 2008, **133**, 403–414.
8 O. Attree, I. M. Olivos, I. Okabe, L. C. Bailey, D. L. Nelson, R. A. Lewis, R. R. McInnes and R. L. Nussbaum, *Nature*, 1992, **358**, 239–242.
9 J. Laporte, L. J. Hu, C. Kretz, J. L. Mandel, P. Kioschis, J. F. Coy, S. M. Klauck, A. Poustka and N. Dahl, *Nat. Genet.*, 1996, **13**, 175–182.
10 A. Bolino, M. Muglia, F. L. Conforti, E. LeGuern, M. A. Salih, D. M. Georgiou, K. Christodoulou, I. Hausmanowa-Petrusewicz, P. Mandich, A. Schenone, A. Gambardella, F. Bono, A. Quattrone, M. Devoto and A. P. Monaco, *Nat. Genet.*, 2000, **25**, 17–19.
11 L. Stephens, K. Anderson, D. Stokoe, H. Erdjument-Bromage, G. F. Painter, A. B. Holmes, P. R. Gaffney,

C. B. Reese, F. McCormick, P. Tempst, J. Coadwell and P. T. Hawkins, *Science*, 1998, **279**, 710–714.
12 T. Rohács, J. Chen, G. D. Prestwich and D. E. Logothetis, *J. Biol. Chem.*, 1999, **274**, 36065–36072.
13 B. Olety, S. L. Veatch and A. Ono, *J. Virol.*, 2015, **89**, 7861–7873.
14 R. Ghai, X. Du, H. Wang, J. Dong, C. Ferguson, A. J. Brown, R. G. Parton, J. W. Wu and H. Yang, *Nat. Commun.*, 2017, **8**, 757.
15 J. M. Bryant, M. M. Malabanan, B. H. Vanderloop, C. M. Nichols, Z. Haratipour, K. T. Poon, S. D. Sherrod, J. A. McLean and R. D. Blind, *J. Lipid Res.*, 2021, **62**, 100081.
16 L. Borges-Araújo, M. M. Domingues, A. Fedorov, N. C. Santos, M. N. Melo and F. Fernandes, *Commun. Chem.*, 2021, **4**, 164.
17 T. Nishimura, M. Gecht, R. Covino, G. Hummer, M. A. Surma, C. Klose, H. Arai, N. Kono and C. J. Stefan, *Mol. Cell*, 2019, **75**, 1043–1057.e8.
18 V. Chan, C. Camardi, K. Zhang, L. A. Orofiamma, K. E. Anderson, J. Hoque, L. N. Bone, Y. Awadeh, D. K. C. Lee, N. J. Fu, J. T. S. Chow, L. Salmena, L. R. Stephens, P. T. Hawkins, C. N. Antonescu and R. J. Botelho, *Mol. Biol. Cell*, 2024, **35**, ar118.
19 J. Edwards-Hicks, P. Apostolova, J. M. Buescher, H. Maib, M. A. Stanczak, M. Corrado, R. I. Klein Geltink, M. E. Maccari, M. Villa, G. E. Carrizo, D. E. Sanin, F. Baixauli, B. Kelly, J. D. Curtis, F. Haessler, A. Patterson, C. S. Field, G. Caputa, R. L. Kyle, M. Soballa, M. Cha, H. Paul, J. Martin, K. M. Grzes, L. Flachsmann, M. Mitterer, L. Zhao, F. Winkler, D. A. Rafei-Shamsabadi, F. Meiss, B. Bengsch, R. Zeiser, D. J. Puleston, D. O'Sullivan, E. J. Pearce and E. L. Pearce, *Nat. Immunol.*, 2023, **24**, 516–530.
20 A. Naguib, G. Bencze, D. D. Engle, I. I. Chio, T. Herzka, K. Watrud, S. Bencze, D. A. Tuveson, D. J. Pappin and L. C. Trotman, *Cell Rep.*, 2015, **10**, 8–19.
21 A. Koizumi, S. Narita, H. Nakanishi, M. Ishikawa, S. Eguchi, H. Kimura, S. Takasuga, M. Huang, T. Inoue, J. Sasaki, T. Yoshioka, T. Habuchi and T. Sasaki, *Sci. Rep.*, 2019, **9**, 13257.
22 R. M. Epand, *J. Membr. Biol.*, 2017, **250**, 353–366.
23 H. Guillou, L. R. Stephens and P. T. Hawkins, *Methods Enzymol.*, 2007, **434**, 117–130.
24 Y. Irino, E. Tokuda, J. Hasegawa, T. Itoh and T. Takenawa, *J. Lipid Res.*, 2012, **53**, 810–819.
25 J. B. Morris, K. A. Hinchliffe, A. Ciruela, A. J. Letcher and R. F. Irvine, *FEBS Lett.*, 2000, **475**, 57–60.
26 G. Chicanne, S. Severin, C. Boscheron, A. D. Terrisse, M. P. Gratacap, F. Gaits-Iacovoni, H. Tronchère and B. Payrastre, *Biochem. J.*, 2012, **447**, 17–23.
27 M. Pulfer and R. C. Murphy, *Mass Spectrom. Rev.*, 2003, **22**, 332–364.
28 M. R. Wenk, *Cell*, 2010, **143**, 888–895.
29 P. Michelsen, B. Jergil and G. Odham, *Rapid Commun. Mass Spectrom.*, 1995, **9**, 1109–1114.
30 F. F. Hsu and J. Turk, *J. Am. Soc. Mass Spectrom.*, 2000, **11**, 986–999.
31 M. R. Wenk, L. Lucast, G. Di Paolo, A. J. Romanelli, S. F. Suchy, R. L. Nussbaum, G. W. Cline, G. I. Shulman, W. McMurray and P. De Camilli, *Nat. Biotechnol.*, 2003, **21**, 813–817.
32 S. B. Milne, P. T. Ivanova, D. DeCamp, R. C. Hsueh and H. A. Brown, *J. Lipid Res.*, 2005, **46**, 1796–1802.
33 T. R. Pettitt, S. K. Dove, A. Lubben, S. D. Calaminus and M. J. Wakelam, *J. Lipid Res.*, 2006, **47**, 1588–1596.
34 H. Ogiso and R. Taguchi, *Anal. Chem.*, 2008, **80**, 9226–9232.
35 J. Clark, K. E. Anderson, V. Juvin, T. S. Smith, F. Karpe, M. J. Wakelam, L. R. Stephens and P. T. Hawkins, *Nat. Methods*, 2011, **8**, 267–272.
36 S. H. Kim, H. E. Song, S. J. Kim, D. C. Woo, S. Chang, W. G. Choi, M. J. Kim, S. H. Back and H. J. Yoo, *J. Lipid Res.*, 2017, **58**, 469–478.
37 C. Wang, J. P. Palavicini, M. Wang, L. Chen, K. Yang, P. A. Crawford and X. Han, *Anal. Chem.*, 2016, **88**, 12137–12144.
38 H. H. Bui, P. E. Sanders, D. Bodenmiller, M. S. Kuo, G. P. Donoho and A. S. Fischl, *Anal. Biochem.*, 2018, **547**, 66–76.
39 M. Malek, A. Kielkowska, T. Chessa, K. E. Anderson, D. Barneda, P. Pir, H. Nakanishi, S. Eguchi, A. Koizumi, J. Sasaki, V. Juvin, V. Y. Kiselev, I. Niewczas, A. Gray, A. Valayer, D. Spensberger, M. Imbert, S. Felisbino, T. Habuchi, S. Beinke, S. Cosulich, N. Le Novère, T. Sasaki, J. Clark, P. T. Hawkins and L. R. Stephens, *Mol. Cell*, 2017, **68**, 566–580.e10.
40 P. Li and M. Lämmerhofer, *Anal. Chem.*, 2021, **93**, 9583–9592.
41 S. Morioka, H. Nakanishi, T. Yamamoto, J. Hasegawa, E. Tokuda, T. Hikita, T. Sakihara, Y. Kugii, C. Oneyama, M. Yamazaki, A. Suzuki, J. Sasaki and T. Sasaki, *Nat. Commun.*, 2022, **13**, 83.
42 Y. Shimanaka, K. Matsumoto, Y. Tanaka, Y. Ishino, S. Ni, J. Guan, H. Arai and N. Kono, *Commun. Chem.*, 2022, **5**, 61.
43 Y. Ishino, Y. Kishi, T. Iwama, N. Kuwayama, H. Arai, Y. Gotoh, J. Aoki and N. Kono, *bioRxiv*, 2024, preprint, 2024.04.30.588048, DOI: **10.1101/2024.04.30.588048**.
44 H. C. Lee, T. Inoue, R. Imae, N. Kono, S. Shirae, S. Matsuda, K. Gengyo-Ando, S. Mitani and H. Arai, *Mol. Biol. Cell*, 2008, **19**, 1174–1184.
45 I. Tang, A. Nisal, A. Reed, T. B. Ware, A. Johansen, M. S. Zaki, B. F. Cravatt and J. G. Gleeson, *Sci. Transl. Med.*, 2025, **17**, eadp5247.
46 H. C. Lee, T. Inoue, J. Sasaki, T. Kubo, S. Matsuda, Y. Nakasaki, M. Hattori, F. Tanaka, O. Udagawa, N. Kono, T. Itoh, H. Ogiso, R. Taguchi, M. Arita, T. Sasaki and H. Arai, *Mol. Biol. Cell*, 2012, **23**, 4689–4700.
47 K. E. Anderson, A. Kielkowska, T. N. Durrant, V. Juvin, J. Clark, L. R. Stephens and P. T. Hawkins, *PLoS One*, 2013, **8**, e58425.
48 Y. V. Shulga, R. A. Anderson, M. K. Topham and R. M. Epand, *J. Biol. Chem.*, 2012, **287**, 35953–35963.
49 N. Steinfeld, S. S. P. Giridharan, E. J. Kauffman and L. S. Weisman, *Methods Mol. Biol.*, 2021, **2251**, 1–17.

50 D. Sarkes and L. E. Rameh, *Biochem. J.*, 2010, **428**, 375–384.
51 M. Fujii, S. Kita, M. Hirata and T. Iwamoto, *Nihon Yakurigaku Zasshi*, 2013, **142**, 236–240.
52 D. Gode and D. A. Volmer, *Analyst*, 2013, **138**, 1289–1315.
53 M. K. Passarelli and A. G. Ewing, *Curr. Opin. Chem. Biol.*, 2013, **17**, 854–859.
54 N. Li, P. Wang, X. Liu, C. Han, W. Ren, T. Li, X. Li, F. Tao and Z. Zhao, *Anal. Chem.*, 2019, **91**, 15873–15882.
55 K. C. Pathmasiri, M. R. Pergande, F. Tobias, R. Rebiai, A. Rosenhouse-Dantsker, E. R. Bongarzone and S. M. Cologna, *J. Lipid Res.*, 2020, **61**, 1004–1013.
56 F. Lanucara, S. W. Holman, C. J. Gray and C. E. Eyers, *Nat. Chem.*, 2014, **6**, 281–294.